Supplement of Atmos. Meas. Tech., 17, 3697–3718, 2024
https://doi.org/10.5194/amt-17-3697-2024-supplement


Atmospheric Measurement Techniques
Open Access
EGU

*Supplement of*

# Cost-effective off-grid automatic precipitation samplers for pollutant and biogeochemical atmospheric deposition

**Alessia A. Colussi et al.**

*Correspondence to:* Trevor C. VandenBoer (tvandenb@yorku.ca)

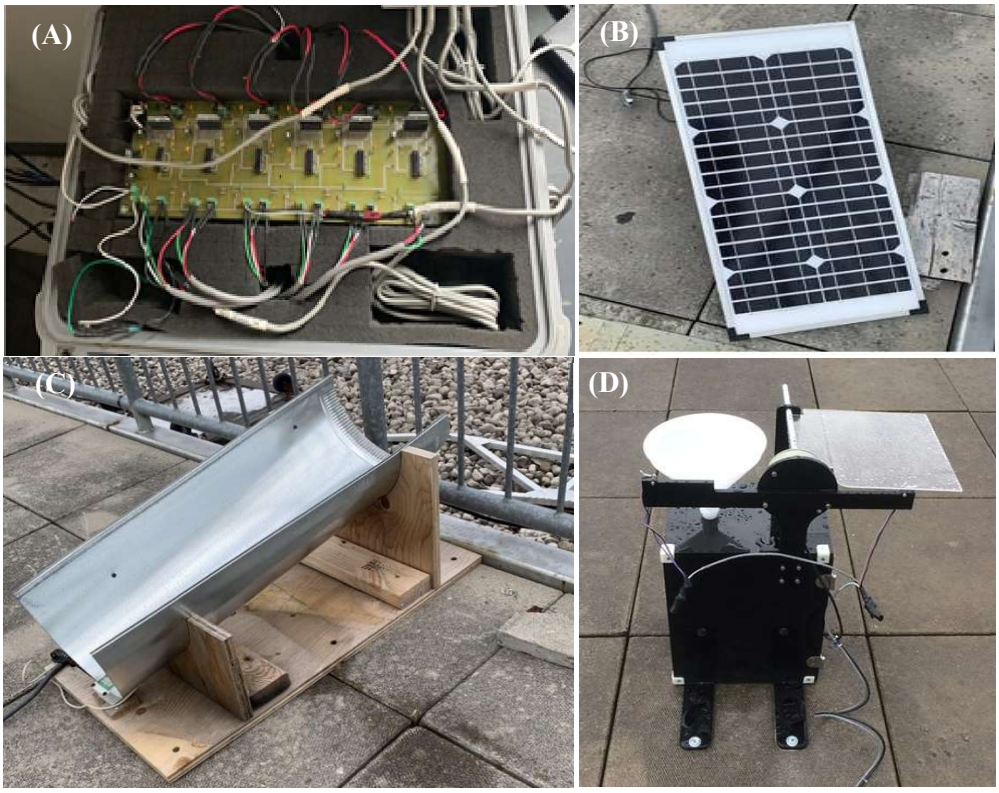


**Figure S1.** Automated precipitation array stationed at the Air Quality Research Station, York University, Toronto, consisting of: **(A)** weather-proofed control board, **(B)** 40 W solar panel, **(C)** rain sensor, and enhanced sensitivity chute, and **(D)** an automated collection unit fixed to concrete with lag sleeves and bolts during a rain event.

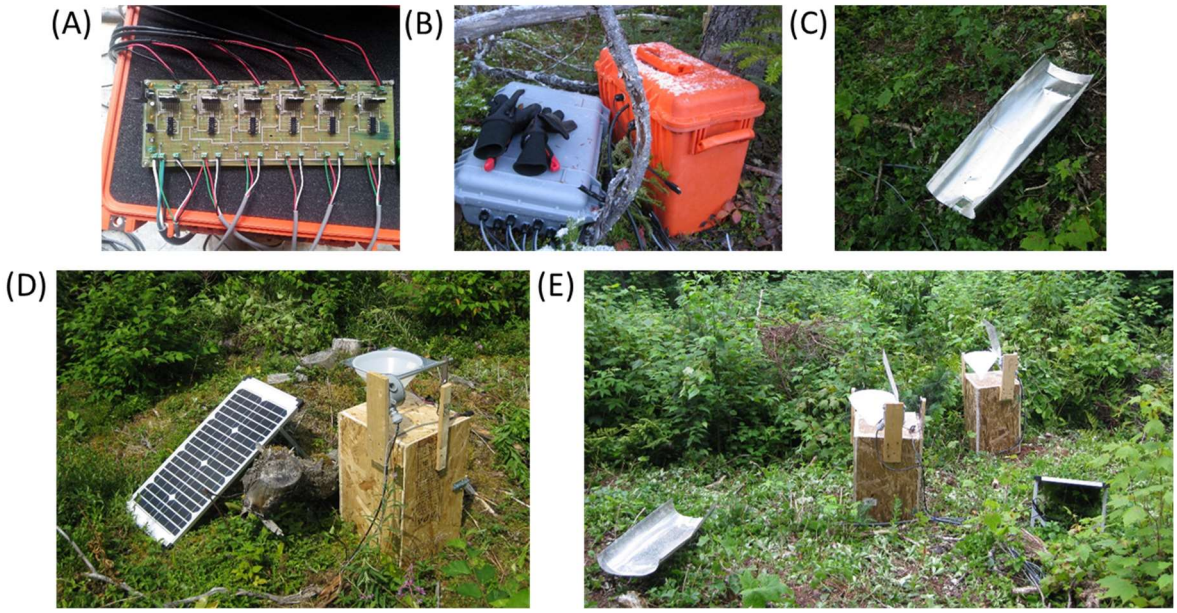


**Figure S2.** Automated precipitation samplers deployed at NL-BELT. The **(A)** weatherproof control board was powered by **(B)** an off-grid AGM battery. The **(C)** sensor chute modulated the opening of the samplers for precipitation collection with **(D)** a 40 W solar panel to recharge the power package between **(E)** precipitation events when the lids open to collect wet deposition.

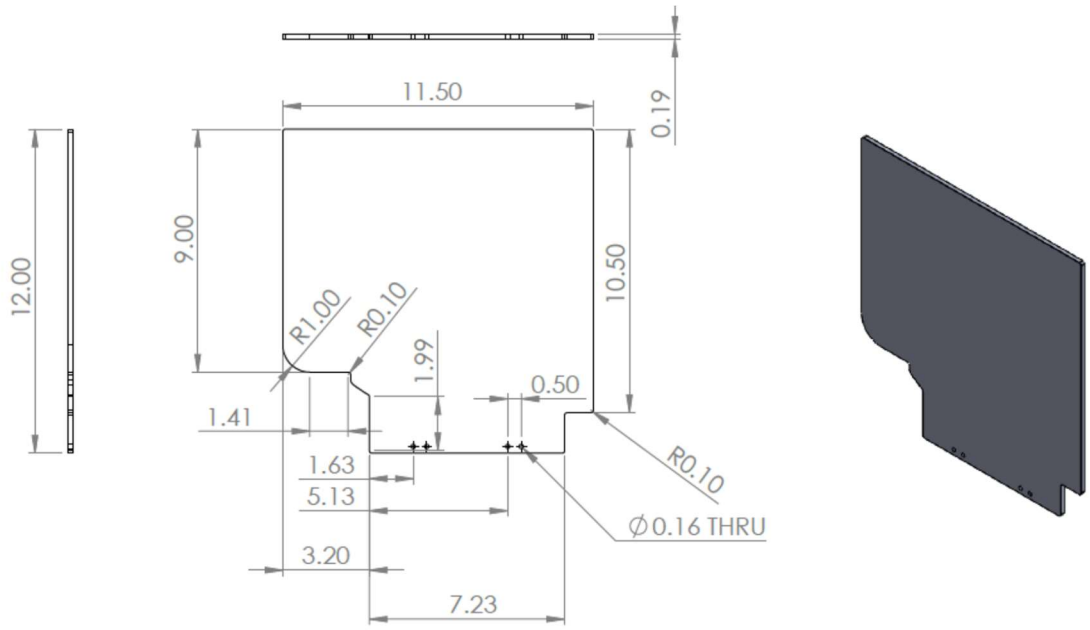


**Figure S3.** Dimensions (in inches; where 1 in. is equivalent to 2.54 cm) for automated collection unit lid, with mounting holes on the bottom edge to secure it to the aluminum lid rod.

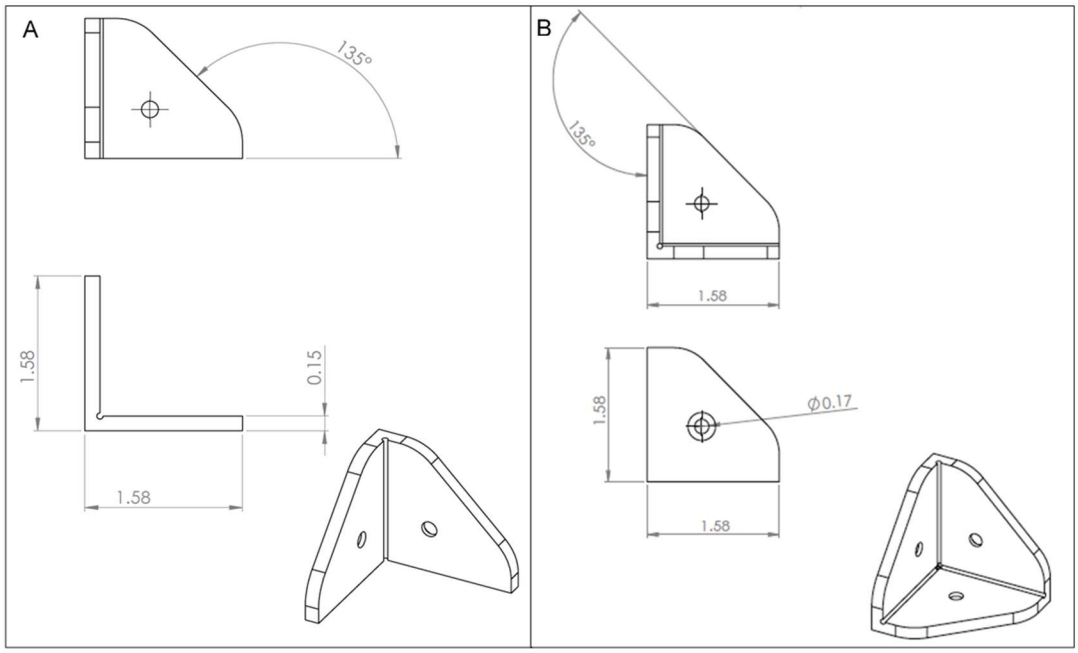


**Figure S4.** Dimensions (in millimeters) of 3D printed corner options: **(A)** double corner to affix panels adjoining the door and **(B)** multi corner used to secure three panels throughout the remainder of the collection unit.

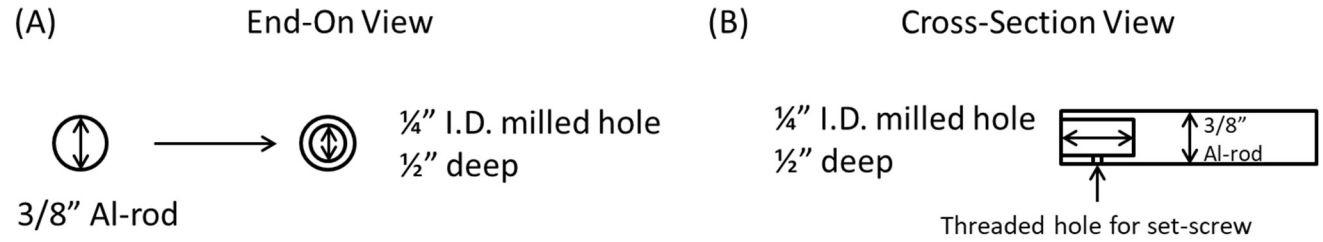


**Figure S5.** Aluminum rod milling schematics showing **(A)** end-on view for motor drive shaft and **(B)** cross section for situating the setscrew to hold the rod to the drive shaft of the motor. All dimensions are in inches where 1 in. is equivalent to 2.54 cm.

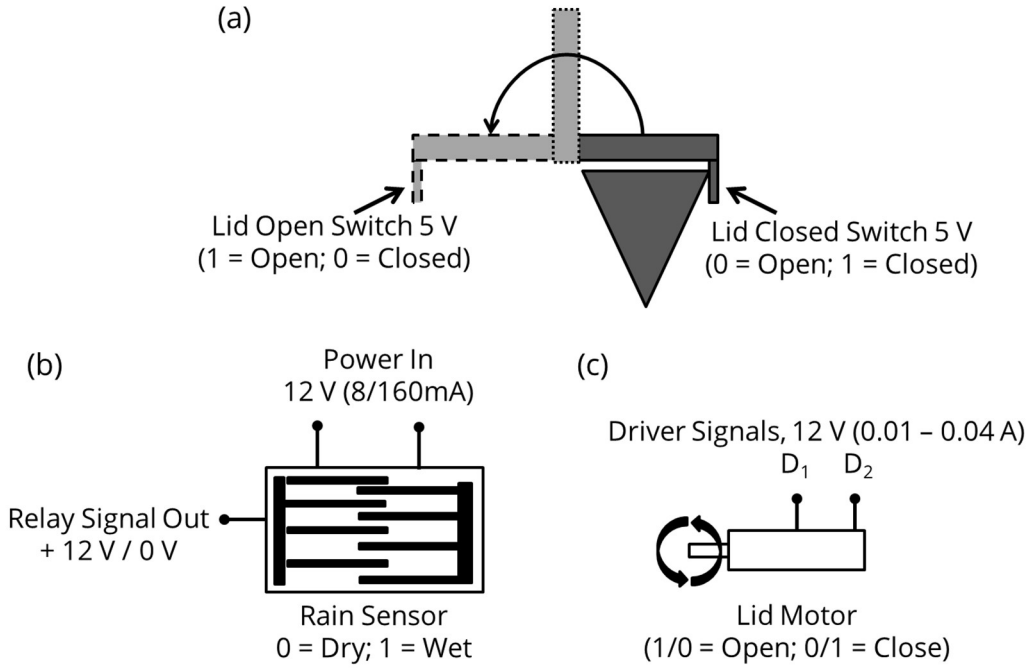


**Figure S6.** Voltage and logic states of the **(a)** lid switches, **(b)** precipitation sensor, and **(c)** lid motor used to drive digital decision making on custom control boards.

(a)

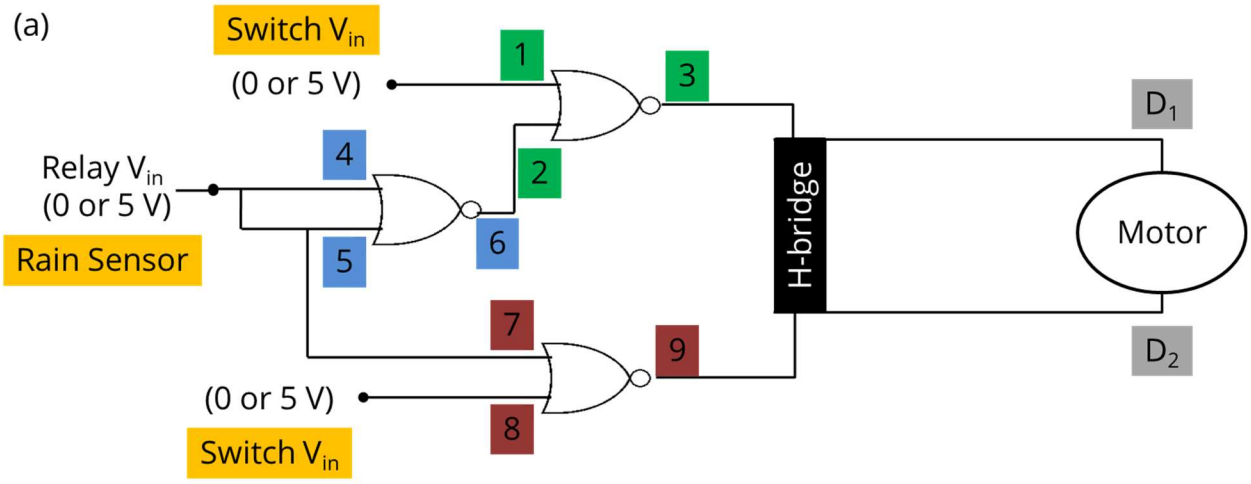


(b)

| Switch | Switch | Rain | 1 | 2 | 3 | 4 | 5 | 6 | 7 | 8 | 9 | D1 | D2 |
|---|---|---|---|---|---|---|---|---|---|---|---|---|---|
| 1 | 1 | 1 | X | X | X | X | X | X | X | X | X | X | X |
| 1 | 1 | 0 | X | X | X | X | X | X | X | X | X | X | X |
| 1 | 0 | 1 | 1 | 0 | 0 | 1 | 1 | 0 | 1 | 0 | 0 | 0 | 0 |
| 1 | 0 | 0 | 1 | 1 | 0 | 0 | 0 | 1 | 0 | 0 | 1 | 0 | 1 |
| 0 | 1 | 1 | 0 | 0 | 1 | 1 | 1 | 0 | 1 | 1 | 0 | 1 | 0 |
| 0 | 1 | 0 | 0 | 1 | 0 | 0 | 0 | 1 | 0 | 1 | 0 | 0 | 0 |
| 0 | 0 | 1 | 0 | 0 | 1 | 1 | 1 | 0 | 1 | 0 | 0 | 1 | 0 |
| 0 | 0 | 0 | 0 | 1 | 0 | 0 | 0 | 1 | 0 | 0 | 1 | 0 | 1 |

**Figure S7. (a)** Input layout for digital logic control of precipitation sampler using three NOR gates to operate a H-bridge motor driver and **(b)** corresponding truth table to input and output logic states for switches and rain sensor (yellow), first NOR gate (green), second NOR gate (blue), and third NOR gate (red) to control 12 VDC from the motor driver to the motor terminals ($D_1$ and $D_2$).

**S1. Measuring conductivity threshold of Kemo electronic rain sensor.**

A simple procedure determined the conductivity threshold of the 12 VDC Kemo Electronic rain sensor. A 1000 µS/cm stock standard was prepared by dissolving 0.225 g of sodium chloride in 500 mL deionized water, ensuring thorough mixing for homogeneity. A series of conductivity standards were then prepared by diluting the stock standard with deionized water (DIW) to different levels near the suspected threshold of the sensor (0.75, 0.8, 0.9, 1.0, 2.0, 3.0, 4.0, and 5.0 µS/cm). Prior to this testing, the rain sensor was flushed with copious amount of DIW to remove any conductive substance from the surface of the sensor - this was also repeated in between trials. The result from testing with these solutions determined that the conductivity threshold for the relay is 1.0 µS/cm, as the rain sensor was observed to be only partially activated at 0.9 µS/cm and the result was not consistent.

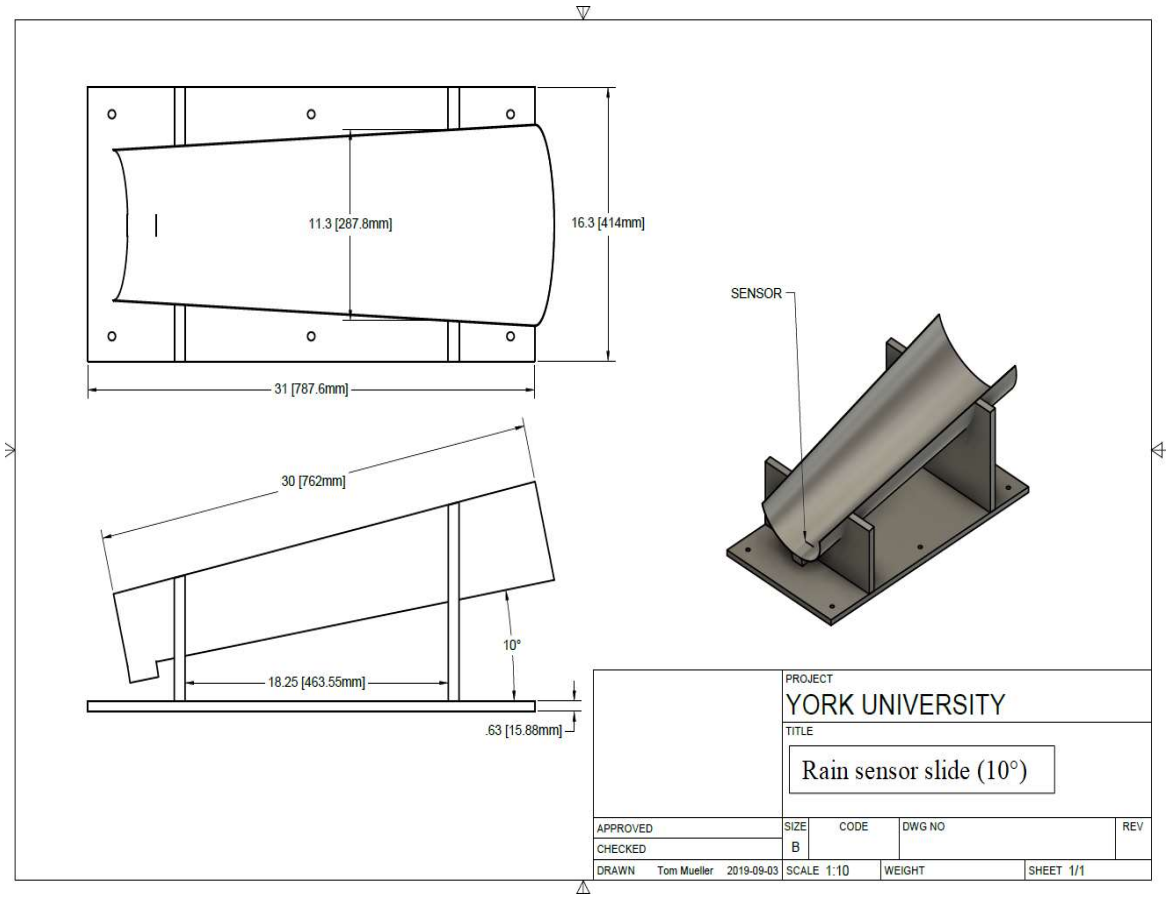


**Figure S8.** Design and dimensions (in mm) of the mounting chute for the rain sensor. The chute slope is fixed at an optimized angle of 10°, that maintains water on the surface of the sensor throughout a rain event but allows excess water to flow over the sensor when necessary. We also tested 15° and 20° through manual observation but found that rainwater would flow over the sensor too rapidly – limiting or even preventing detection of wet deposition events.

(a)

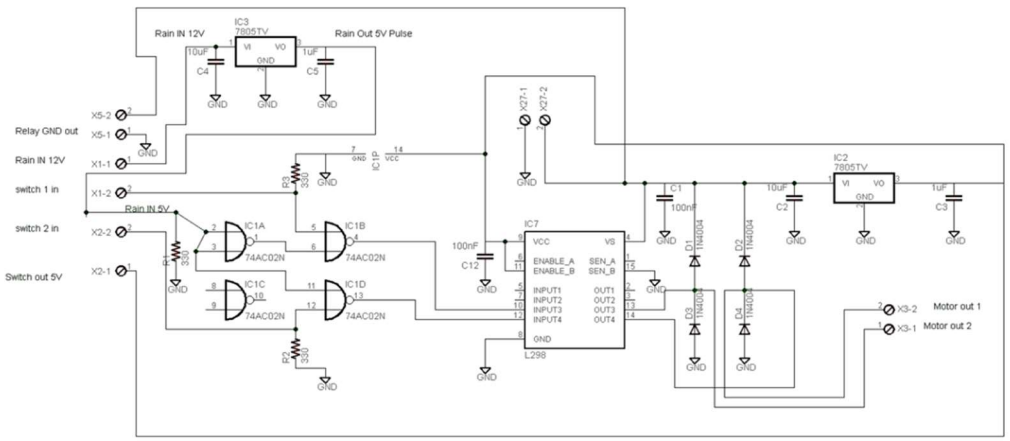


(b)

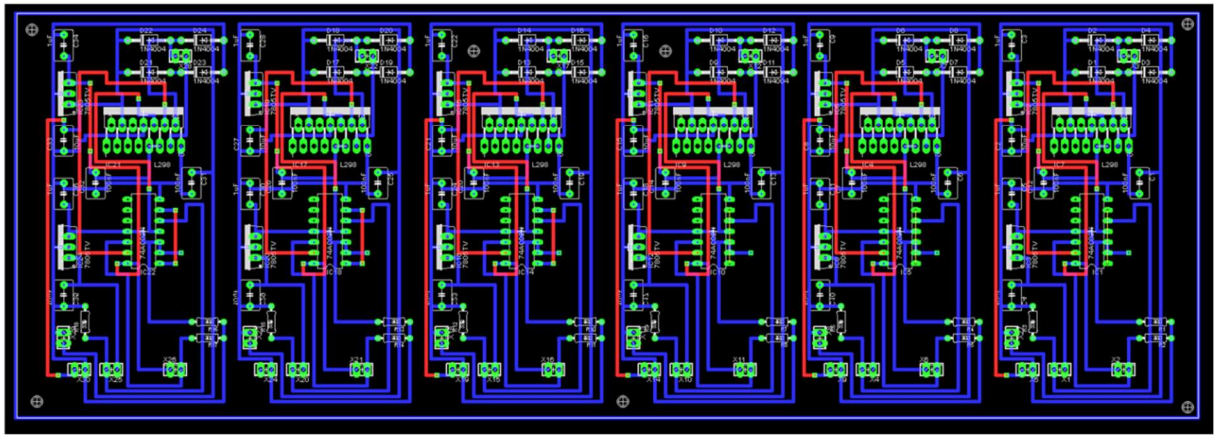

**Figure S9.** Technical schematics for all printed circuit board components required to control **(a)** one precipitation collector with all components and connections to chips indicated and **(b)** a complete six-unit array composed of replicate layouts.

**Table S1.** List of required components, part numbers, and quantities required to assemble a single printed circuit board.

| Component | Part Identification | Description | Quantity | Unit Price (CAD) |
|---|---|---|---|---|
| Integrated Circuit 1 (IC1) | 74AC02N = SN7402n | Four channels, two input NOR gate | 1 | 3.52 |
| Integrated Circuit 7(IC7) | L298N | Dual Full Bridge Driver | 1 | 7.41 |
| Integrated Circuit 2 (IC2), Integrated Circuit 3 (IC3) | 7805TV = MC7805CT-BP | 5V regulator, TO220 | 2 | 0.67 |
| Diode 1, Diode 2, Diode 3, Diode 4 | 1N4004 | Diode | 4 | 0.14 |
| Resistor 1, Resistor 2, Resistor 3 | 10k | resistor, %1, 1/4W | 3 | 0.21 |
| Capacitor 1, Capacitor 12 | 100nF cap | Capacitor, 0.1Uf / 50V | 2 | 0.35 |
| Capacitor 3, Capacitor 5 | 1Uf Cap | Capacitor, 1UF, 50V | 2 | 0.84 |
| Capacitor 2, Capacitor 4 | 10Uf | Capacitor, %10,10Uf,50V | 2 | 1.84 |

**Table S2.** List of specific components, manufacturers, and specifications required to construct precipitation collection arrays. Note that 1 in. is equivalent to 2.54 cm.

| Components | Description | Selection Rationale |
|---|---|---|
| | **Collection Units** | |
| Boxes | **Material:** 3/8" Acrylic or Plywood<br>**Dimensions:** (33.78 W x 33.78 L x 42.94 H) cm<br>See Figure 2 for more details | Acrylic and plywood were chosen for their low cost and durability against a variety of environmental conditions. Both materials are opaque to minimize light intrusion. |
| Collection Container | **Material:** High Density Polyethylene<br>**Brand:** Bel-Art Products<br>**Dimensions:** (19 H x 26 W x 36 H) cm; **Volume**: 10 L | Large volume collection of precipitation and resistance of material to environmental degradation. Quantitatively transfers analytes such as inorganic ions and DOC. |
| Funnel | **Material:** High Density Polyethylene<br>**Brand:** Dynalon<br>**Dimensions:** 9.4" W x 8.68" H; 20 cm diameter | Guides conductive precipitation into the collection container. Material is matched to maintain quantitative analyte transfer. |
| Sampler Lids | **Materials:** Lexan<br>**Brand:** Kraloy, Carlon® Lamson & Sessions<br>**Dimensions:** See Figure S3 for more details<br>**Voltage:** 12 V | Prevents foreign material entering the collection container when closed. Lexan was chosen due to its high flexibility and impact resistance. Acrylic was determined to be too fragile and not suitable for environmental conditions with elevated winds. |
| Geared Box DC Motor | **Brand:** Tsiny Motor Industrial Co. Ltd. TS-32GZ370-1650<br>**Operating voltage range**: 6-24 VDC<br>**Nominal voltage:** 12 VDC **Speed:** 2-8 RPM | The worm gear motor is connected to the aluminum rod and sampler lids to open and close them when conductive precipitation is detected by the rain sensor. |

**Table S2 (cont'd).** List of specific components, manufacturers, and specifications required to construct precipitation collection arrays.

| Components | Description | Selection Rationale |
|---|---|---|
| | **Collection Units (cont'd)** | |
| Lid Rod | **Material:** Aluminum<br>**Outer diameter:** 3/8"<br>**Inner diameter:** 1/4"<br>**Depth:** 1/2" deep | The aluminum rod is attached to the motor and facilitates the opening and closing of the Lexan lids. The rod is attached to the motor by a 8/32 threaded 1/4" set screw. |
| Lid Limit Switches | **Brand:** Omron Electronics<br>**Part Number:** D2FW-G271M(D)<br>**Max Current:** 1 A | Snap action switches are used to detect the open and closed position of the motorized sampler lids. Weatherproofing keeps them watertight. |
| Funnel Mesh | **Material:** HDPE<br>**Brand:** McMaster-Carr<br>**Part Number:** 9265T49 | When the automated sampler is in the open position, these cone-shaped filters prevent debris from entering the collection jug. |
| Lag shields, lag bolts and washers | **Lag shields dimensions:** 3/8" x 1-3/4"<br>(Requires masonry drill bit: 5/8")<br>**Lag bolt and washer dimensions:** 1/2" | These are utilized to secure precipitation collectors to concrete. This prevents unit tipping during storms or from animal interactions.<br>Tent pegs or rebar may be alternatively used to secure the samplers into soils. |
| | **Power System** | |
| Solar Panel | **Brand:** Coleman 40W Folding Panel<br>**Output Voltage:** 17.1 V, 2.3 amps<br>**Dimensions:** (79 L x 35.1 W x 1.8 H) cm | The solar panel recharges the off-grid battery. This can be repositioned to optimize sunlight exposure and maximize recharging capabilities. |

**Table S2 (cont'd).** List of specific components, manufacturers, and specifications required to construct precipitation collection arrays.

| Components | Description | Selection Rationale |
|---|---|---|
| | **Power System (cont'd)** | |
| Solar Charge Controller | **Brand:** Coleman<br>**Load Charge:** 8.5 A<br>**Cut-out:** 14.2 V<br>**Cut-in:** 13 V | The ability of the solar panel to deliver charge to the battery or stop when it is fully charged is regulated. The controller prevents the battery from overcharging. |
| 103 Ah off-grid battery | **Brand:** Motomaster Nautilus Ultra XD Group 31 High Performance AGM Deep Cycle Battery (103 Ah)<br>**Voltage:** 12 V<br>**Dimensions:** (33 L x 18 W x 25 H) cm | The 99.99% lead AGM (absorbed glass mat) was used for long lasting power and reliability for field testing without a solar panel. |
| 76 Ah Off-grid battery | **Brand:** Motomaster Nautilus Ultra XD Group 24 High Performance AGM Deep Cycle Battery (76 Ah)<br>**Voltage:** 12 V<br>**Dimensions:** (27.6 L x 17.1 W x 22.2 H) cm | The 99.99% lead AGM with 76 Ah battery was used for field testing while being charged with a solar panel for long periods. |
| Transformer | **Brand:** TDK Lambda Americas<br>**Voltage:** 115 VAC to 12 VDC | The transformer replaces an off-grid battery and converts 115 VAC to 12 VDC. This can be used when sampling in locations with grid power available. |

**Table S2 (cont'd).** List of specific components, manufacturers, and specifications required to construct precipitation collection arrays.

| Components | Description | Selection Rationale |
|---|---|---|
| | **Rain Detection** | |
| Heated Precipitation Sensor | Brand: Kemo Electronic M152<br>Voltage: 12 V<br>Dimensions: (6.5 x 4.5 x 3.6) cm | A waterproof conductive sensor that becomes activated and switches on a relay when in contact with conductive rain or snow. The sensor relay triggers the control board so that the sampler lids rotate open. The operating temperature range provided by the manufacturer is -10 to +55°C. |
| Sensor Chute | **Dimensions:** (see Figure S8) | Increases surface area of precipitation sensor to activate the relay. Delays lid closing by providing more conductive ions to the sensor surface when atmospheric wash out may occur. |
| | **Digital Control Board** | |
| Control Boards | See Figure S9 for more details. | Controls communication between the motors, power supply, and rain sensor (12 VDC), as well as the two limit switches (5 VDC). |
| Control Board Protective Case | **Brand:** Pelican ™ 1450 Case<br>**Material of body:** polypropylene<br>**Exterior Dimensions: (**41.8 L x 33 W x 17.3 D) cm<br>**Interior Dimensions:** (37.2 L x 26 W x 15.5 D) cm<br>**Weight with foam (polyurethane):** 2.9 kg | The 1450 case contains custom foam for cable accommodations with automatic pressure equalization valve to balance interior pressure. It is watertight, crushproof, and dustproof with double throw latches and a rubber handle. |
| Reusable Hydrosorbent Silica Gel Beads | **Brand:** Pelican Case Desiccant<br>**Canister Dimensions: (**1.3 L x 5.1 W x 10.2 H) cm<br>**Mass:** 40 g | The silica gel beads absorb moisture to prevent water damage to the control board; when clear, must reactivate in an oven for 3 hours at 300°F. |

**Table S2 (cont'd).** List of specific components, manufacturers, and specifications required to construct precipitation collection arrays.

| Components | Description | Selection Rationale |
|---|---|---|
| | **Miscellaneous** | |
| Data logger | **Brand**: ONSET® HOBO 4-channel analog data logger<br>**Part #:** UX120-006M<br>**Program:** HOBOware | To collect and offload data from the control board using one of four channels. This work: CH1 – battery voltage, CH2 – motor driver voltage, CH3 – rain sensor voltage, CH4 – limit switch voltage. |
| Cable Connectors | **Brand:** Bulgin (400 or 4000 Series Buccaneer) IP68 Sealed Electrical Circular Cable Connectors<br>PXP4010/03P/3540 and PSP4011/03S/3540<br>PSP4010/08P/3540 and PSP4011/08S/3540<br>SA3349, SA3350, SA3348, SA3347<br>**Material:** Polyamide UL94-V0 body, gold contacts<br>**Cable acceptance:** 3 mm – 7 mm<br>**Contact insertion:** crimp or solder | Waterproof and dustproof cable connectors provide electrical connections from the control board to the battery, solar panel, and sampler motors and switches. Different numbers of contacts represent different cable requirements within the system (2- or 3-contact = battery and solar panel cables, 6- or 8-contact = rain samplers). |
| Extension Cables | Any commercial outdoor-rated extension cord | To increase distance from VAC power source to sampling location. |

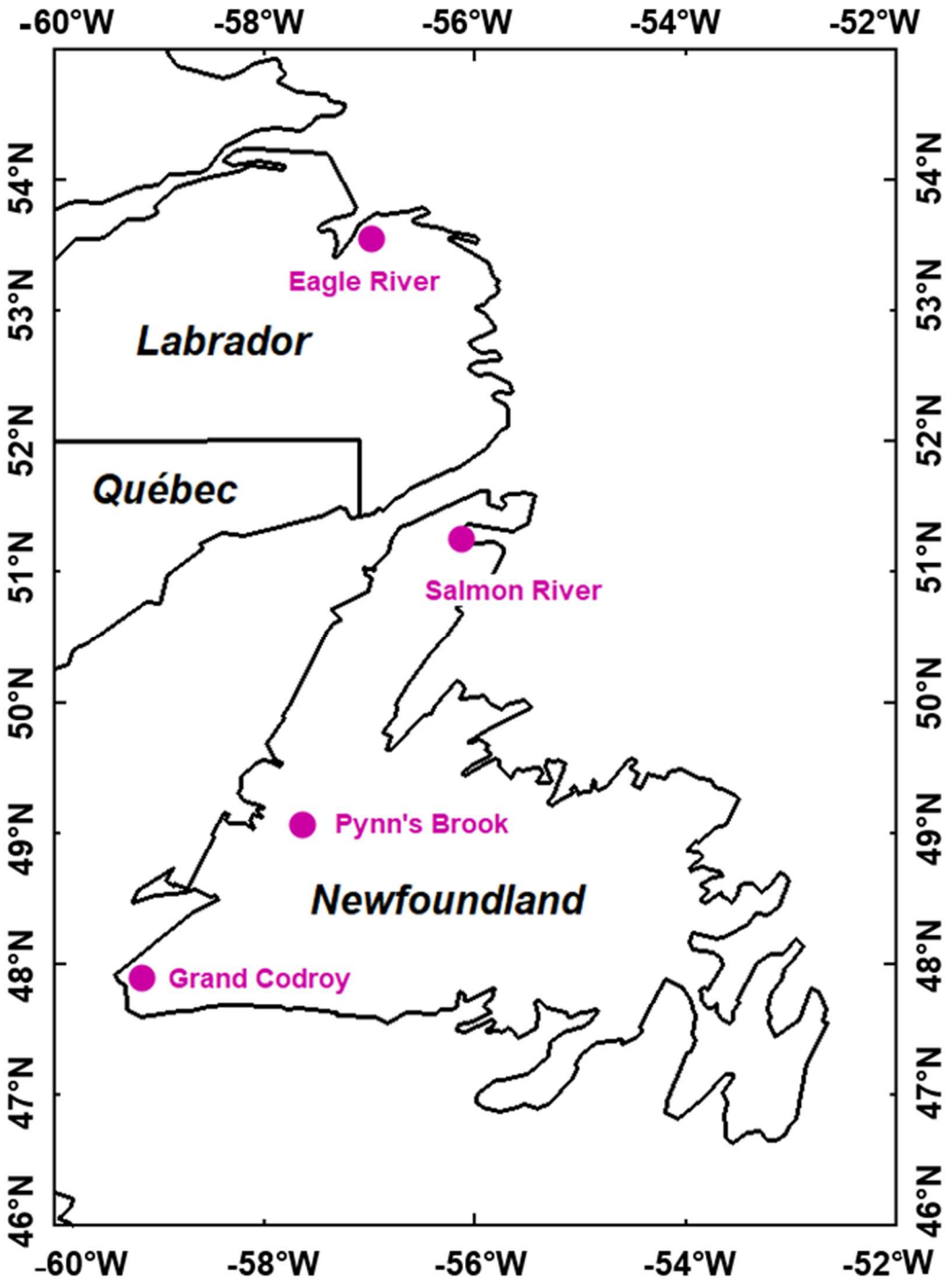


**Figure S10.** Map of the NL-BELT highlighting the four watershed regions where sampling occurred: Grand Codroy (GC), Pynn's Brook (PB), Salmon River (SR), and Eagle River (ER).

**S2. Deposition comparison: this work, DAYMET, and ECCC**

Sufficiently continuous measurements from ECCC stations near each site are challenging to obtain for the 2015-16 period. When available with greater than 80% coverage, the ECCC datasets both agree and disagree with our observations in GC and SR, respectively, suggesting that there is substantial deposition volume heterogeneity at the scale of ~10 km in this region. In SR, the disagreement with our measurements is identical to the DAYMET model which uses ECCC observations as input data, while at GC the ECCC measurements are identical to ours (Table S3). Further, the discrepancy in the PB or ER average annual precipitation volume between ECCC and those of this work and DAYMET are not possible to interrogate due to the large quantity of data missing from the ECCC monitoring station (35.22% in ER and 39.65% in HR/PB; Table S3). The DAYMET observations are representative of a larger spatial scale, where our discrete samplers could be subject to heterogeneity in deposition (e.g., orographic precipitation, driven by topography like steep slopes) or impacted by meteorological conditions not captured by the model (e.g., undercatch driven by local winds). The temporally resolved volume comparisons at sampling interval timescales better-demonstrates comparability, despite the systematic differences. The month-to-month relationships between DAYMET and our observations, as well as between ECCC and our observations, all show strong correlations with linear regressions having $R^2$ values, from north to south, of 0.72, 0.99, 0.99, and 0.86, and N/A, 0.94, N/A, and 0.93, respectively (Table S3). The discrepancy between DAYMET, ECCC, and our observations for total deposition were highest in the most northerly site, where the experimental site was located on a steep slope, with only 43 % of the predicted volume collected. At all of the sample collection sites on the island of Newfoundland, a consistent difference was observed with 65 ± 4 % of the estimated volume collected, except at GC where our measurements and those from ECCC are identical and starkly contrasting to DAYMET. Overall, parsing these comparisons is difficult and demonstrates that there may be up to 55% additional uncertainty in deposited species, should given measurements of a species be scaled for a watershed like ER by concentration in total deposition samples. We propose, that by isolating only the deposited analytes and using analyte fluxes instead of concentrations in precipitation samples, that uncertainty issues in representing volumes, improves overall deposition budget certainties.

**Table S3.** Collected precipitation volumes from NL-BELT in bulk deposition samplers for rainwater were deployed for one to two months, while snow was collected as an integrated sample throughout the winter because sites were not accessible. The Environment and Climate Change Canada (ECCC) precipitation data was obtained for identical sampling intervals. The DAYMET model for North America (1 km x 1 km resolution) for precipitation was obtained for the identical sampling intervals, which utilizes interpolated and extrapolated data from daily weather observations to predict inputs at the NL-BELT locations. Linear regression results for slope (m) and correlation coefficient ($R^2$) between observations and DAYMET (*italics*), and observations and ECCC (where possible; underlined), were calculated. For sampling periods where a measurement was compromised or not collected for a given interval in this work, these are reported as with '-' and an estimated volume from the regression relationship with ECCC is reported in parentheses when used to replace compromised samples.

| Date (mmm-yy) | Grand Codroy | | | Pynn's Brook/ Humber River | | | Salmon River | | | Eagle River | | |
|---|---|---|---|---|---|---|---|---|---|---|---|---|
| | This Work (L) | DAYMET (L) | ECCC (L) | This Work (L) | DAYMET (L) | ECCC (L) | This Work (L) | DAYMET (L) | ECCC (L) | This Work (L) | DAYMET (L) | ECCC (L) |
| Jun-15 | 22.68 | 40.98 | 23.80[b] | 23.44 | 36.94 | 11.47[b] | - | - | - | - | - | - |
| Jul-15 | 2.92 | 3.38 | 2.06 | 2.24 | 2.93 | 1.04[b] | 21.12 | 31.13 | 30.94 | 13.85 | 40.92 | 15.09[b] |
| Aug-15 | 6.86 | 8.08 | 7.20 | 5.06 | 6.86 | - | 1.89 | 4.71 | 9.52 | 3.66 | 6.96 | 2.64[c] |
| Sep-15 | (5.17)[a] | 2.93 | 5.17 | 3.05 | 4.70 | - | 5.29 | 6.62 | 6.44 | - | - | - |
| Oct-15 | 1.71 | 4.31 | 4.44 | - | - | - | 3.62 | 5.20 | 6.18 | - | - | - |
| Nov-15 | 3.57 | 5.92 | 4.92 | 5.66 | 8.61 | - | - | - | - | - | - | - |
| May-16 | 26.00 | 28.15 | 25.38 | 15.62 | 24.18 | 11.22[b] | 16.19 | 22.73 | 25.33 | - | - | - |
| Jun-16 | 1.83 | 4.21 | 3.79 | 4.25 | 4.51 | 2.79 | 2.39 | 3.11 | 3.05[a] | 22.94 | 45.68 | 22.70[b] |
| Jul-16 | 5.81 | 3.96 | 6.10 | 3.13 | 3.80 | 3.19 | 3.68 | 3.26 | - | - | - | - |
| Aug-16 | 5.19 | 4.10 | 3.98 | 4.67 | 6.14 | 4.23 | 3.60 | 5.18 | 3.89[a] | 5.82 | 10.79 | 6.94[b] |
| Sep-16 | 7.79 | 5.17 | 4.06 | 4.97 | 4.04 | - | 4.95 | 5.95 | 6.69 | - | - | - |
| Oct-16 | 5.10 | 6.69 | 5.30 | 5.15 | 5.84 | 3.47[b] | 2.00 | 2.82 | 2.58 | 5.42 | 8.32 | 4.39[b] |
| m, $R^2$ | 0.62, *0.859;* 1.02, 0.934 | | | 0.60, *0.990;* -, - | | | 0.68, *0.987;* 0.67, 0.941 | | | 0.43, *0.719;* -, - | | |

[a]Sample compromised by wildlife-sampler interaction.
[b]These values result from periods where <80% of the observation days report collected data. Partial volumes from the available data are presented.
[c]These values result from periods where <50% of the observation days report collected data. Partial volumes from the available data are presented.

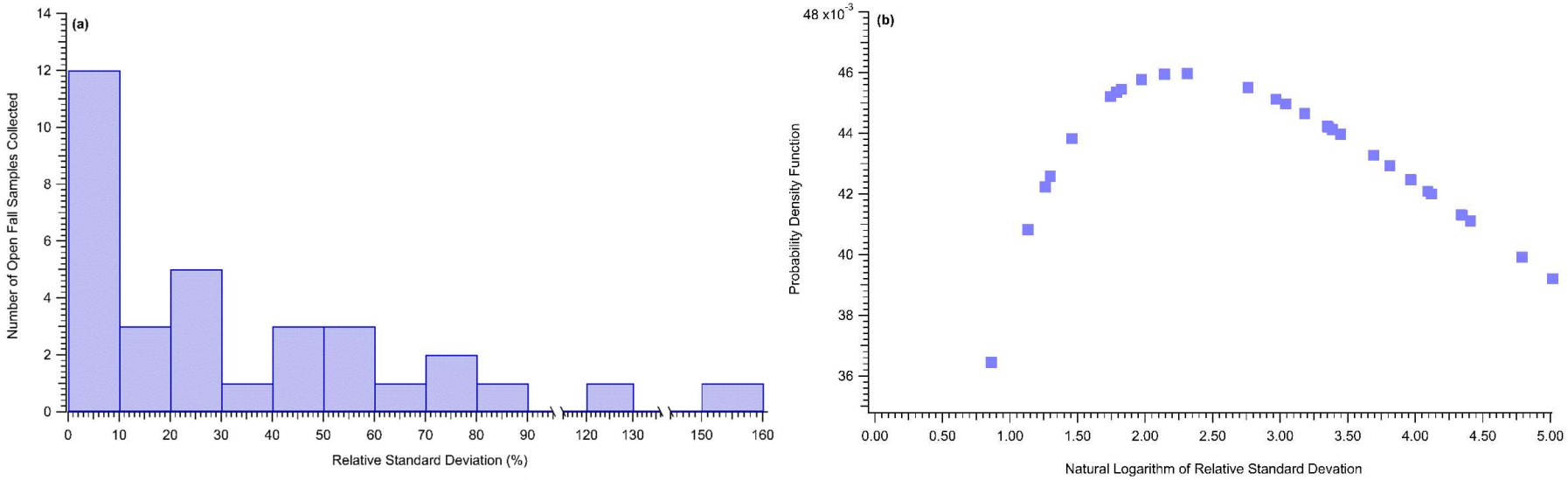


**Figure S11.** Thirty-three sets of triplicate open fall samples were collected across the NL-BELT between 2015 and 2016. **(a)** The replicate relative standard deviations (RSDs) appear to follow a log-normal distribution where reproducibility is typically within ± 12.5% and almost always within ± 31.5%. **(b)** A variable 'x' is said to have a lognormal distribution if y = ln(x) is normally distributed**.** The RSDs were treated as variable 'x' and then log-transformed, resulting in a mean (μ) and standard deviation (σ) of 2.81 and 1.41, respectively. The probability density function for the log-normal, plotted against these log-transformed values, is defined by the two parameters μ and σ, where x > 0. As a result, one of the 33 RSD values was excluded from this plot as it became a negative value after being log-transformed.

**Table S4.** Sum of DOC fluxes (mg C $m^{-2}$ $a^{-1}$) in wet deposition samples for 2015 and 2016 at GC, PB, SR, and ER. The average DOC flux error (mg C $m^{-2}$ $a^{-1}$) propagated by summing the errors across the sampling sites to obtain the annual values.

| | | OF | TF |
|---|---|---|---|
| **Site** | **Year** | **Deposition Flux (mg C $m^{-2}$ $a^{-1}$)** | |
| GC | 2015 | 1800 (± 800) | 3700 (± 2400) |
| | 2016 | 1400 (± 800) | 700 (± 700) |
| PB | 2015 | 600 (± 300) | 1800 (± 600) |
| | 2016 | 7800 (± 7700) | 3000 (± 3600) |
| SR | 2015 | 2000 (± 900) | 3500 (± 2000) |
| | 2016 | 4000 (± 1700) | 1700 (± 1500) |
| ER | 2015 | 100 (± 100) | 1600 (± 2200) |
| | 2016 | 1000 (± 800) | 100 (± 30) |

**Table S5.** Average DOC flux (mg C $m^{-2}$ $a^{-1}$) for 2015 to 2016 at GC, PB, SR, and ER. The difference between calculated fluxes in TF and OF samples are also included.

| | OF | TF | TF - OF |
|---|---|---|---|
| **Site** | **Flux (mg C $m^{-2}$ $a^{-1}$)** | | |
| GC | 1600 | 2200 | 600 |
| PB | 4200 | 2400 | -1800 |
| SR | 3000 | 2600 | 400 |
| ER | 500 | 900 | 400 |